ANNALS OF GEOPHYSICS, 68, 4, DM443, 2025; doi:10.4401/ag-9366
OPEN ACCESS

Multidisciplinary investigation of the Salse di Regnano mud volcanoes (Northern Italy) using remote sensing and historical data

Arianna Pesci[*,1], Giancarlo Tamburello[1], Fabiana Loddo[1], Giordano Teza[2], Zoe Torroni[3], Beatrice Molignini[3]

(1) Istituto Nazionale di Geofisica e Vulcanologia, Sezione di Bologna, Bologna, Italy
(2) Università degli Studi di Bologna, Dipartimento di Fisica e Astronomia, Bologna, Italy
(3) Università degli Studi di Bologna, Dipartimento di Scienze Biologiche, Geologiche e Ambientali, Bologna, Italy

Article history: received May 12, 2025; accepted June 11, 2025

Abstract

This study presents a multidisciplinary analysis of the Salse di Regnano, a significant mud volcanic area in the Emilia-Romagna Apennines, aiming to develop a comprehensive research strategy to investigate its morphological evolution and fluid emission dynamics. High-resolution 3D models generated through UAV-based photogrammetric surveys enabled detailed mapping and monitoring of morphological features, capturing changes over an extended historical period (1907-2025) by integrating regional geological maps and archival topographical data. In-situ measurements of methane (CH_4) and carbon dioxide (CO_2) fluxes revealed localized methane emissions associated with vents characterized by high soil permeability, while CO_2 fluxes likely reflect biogenic soil respiration near mud deposits. However, geochemical signatures, including $\delta^{13}C$-CH_4 values and the presence of ethane, suggest a thermogenic component, highlighting the complex interplay between biological and geological processes governing gas emissions in the area. Complementary satellite imagery and spatial analyses additionally elucidated the spatial distribution of these processes. This multidisciplinary approach not only advances the understanding of mud volcano dynamics in this geologically active region, but also establishes a practical and scalable methodological framework. The proposed workflow, incorporating targeted geophysical surveys such as geomagnetic and passive seismic measurements, aims to enhance the characterization of subsurface structures. As a preliminary study, this contribution provides a valuable foundation for subsequent monitoring and risk assessment efforts of mud volcanic systems in similar geological contexts. In this view, comparing present-day observations with historical data may also offer critical insights for assessing long-term hazard potential.

Keywords: Mud Volcanoes; Photogrammetry; Surface variations; Historical Data, Gas flux

1. Introduction

Mud volcanoes are spectacular and fascinating geological phenomena, surface manifestations of clayey fluids mixed with gases, primarily methane, which rise to the surface through fractures in the ground. Their origin is closely tied to the tectonic and geochemical processes characterizing orogenic areas, where the compression between plates causes the release of muds rich in water and gases trapped in the subsoil. In particular, the formation of the Apennines is the result of the collision between the African and Eurasian plates, which led to the closure of the Tethys Sea and the uplift of the mountain structures. The Emilia Apennines feature a variety of geological units, including the Epiligurian units, the Ligure Flysch, and the limestone and marl formations of the Montefeltro Unit. The pre-Quaternary formations, visible through synclines and anticlines, contain significant accumulations of trapped organic material, which, given specific combinations of temperature and pressure, has been transformed into methane gas and muds. These tectonic processes are complemented by internal chemical phenomena that can lead to the separation of organic components and further increase pressure, promoting the ascent of fluids to the surface. This geochemical process contributes to the formation of mud volcanoes, where the upward movement of gas-rich fluids through tectonic fractures creates the characteristic mud cones.

Emilia-Romagna is one of the Italian regions with the highest concentration of mud volcanoes, so much so that a hiking route known as the "Via dei Vulcani di Fango" (Mud Volcanoes Route) has been established, connecting some of the most significant manifestations of this phenomenon in the area. This route crosses the northern Apennines, a region particularly rich in mud volcanoes that typically form along tectonic fractures associated with fluid upwelling. Among the most prominent examples are the Salse di Nirano, the Salse di Regnano (in the Modena Apennines), and the Salse del Dragone (in the Bologna Apennines). These sites are exemplary cases of active mud volcanoes, thoroughly documented in regional geological maps and extensively investigated in numerous scientific studies (e.g. Bonini et al., 2007; Mazzini and Etiope, 2017). In addition to these well-known sites, the region also hosts other less recognized but still significant manifestations, such as the Salsa di Puianello, the Salse di Castellarano, and the Salse di Baiso. These phenomena, while less documented, remain subjects of study for understanding the variability and evolution of mud volcanoes and are included in regional publications, such as the Geological Map of Italy and reports from local authorities. The Emilia-Romagna Region's website, which shows the distribution of mud volcanoes, provides a very useful service, highlighting the importance of these phenomena not only from a geological perspective but also for the ecosystem services they provide. In particular, the role of mud volcanoes as habitats for biodiversity and their function in regulating the water cycle are emphasized. The approximate location of historically documented mud volcanoes (or groups of mud volcanoes) in Emilia-Romagna, as derived from geological literature (Bonaposta et al., 2018), is shown on the map. The colors indicate the quality of the reports, ranging from green (moderately reliable) to red (with greater uncertainty). Furthermore, activities are underway to verify this data, aiming to create a high-quality informational base for publication on the website's interactive mapping section, accessible through web-GIS. For more information, you can consult the official page of the Emilia-Romagna Region (https://ambiente.regione.emilia-romagna.it).

In the publication Le salse dell'Emilia-Romagna: cartografie a confronto (Bonaposta and De Nardo, 2017), the authors describe the maps created for each group of mud volcanoes, including the mud vents observed in the field and verified through remote sensing images, alignments from which the orientation of fracture systems and deposits can be deduced, and the deposits themselves, mapped or inferred from the morphology. Current data are compared with the original maps of Biasutti (1907) as reported in Dainelli (1907), highlighting the evolution of the phenomena and contributing to refining the local knowledge base for land-use planning.

The comparative analysis between the historical map of the Kingdom of Italy (Regno d'Italia) and the current Regional Technical Map highlights the impact of urban development transformations, with active mud volcanoes now located near urban centers, while others, less affected by such processes, persist in protected and isolated areas. The Salse di Nirano, which are located within a protected natural area, have been subject to a restoration and conservation intervention to preserve their characteristic forms (De Nardo, 2019), while those of Regnano and those of Sassuolo-Montegibbio (still active) are located in more urbanized areas.

Mud volcanoes have been documented since ancient times, with numerous references in the writings of naturalists, geographers, and historians. A significant example dates back to the 18th century, when the renowned scholar Lazzaro Spallanzani, during his travels in the Apennines, described in detail several mud volcanoes in Emilia, hypothesizing their origin through a combination of geological and chemical factors, based on the knowledge of the time (Spallanzani, 1777). His theory, although inaccurate in some parts, marked an important step in the

scientific observation of mud volcanic phenomena. Historical maps, including 19th-century cadastral maps, provide further evidence of the presence of these phenomena, with mud volcanoes indicated as 'mobili terre' or 'unstable lands' (Cadastral Map, 1800). This terminology, used by the geographers of the time, reflected the mysterious and hazardous nature of these areas, often associated with landslides and mass movements. Local chronicles from the time also recount numerous episodes of violent paroxysms, in which the mud volcanoes erupted large amounts of mud and gas, temporarily altering the surrounding landscape (Ferrari, 1876; Bonaposta et al., 2018).

In addition to Emilia-Romagna, mud volcanoes are distributed across other Italian regions, from Piedmont to Sicily. In particular, the Sicilian manifestations are among the most active and spectacular, with phenomena that show similarities to those in Emilia, but often characterized by hotter, more persistent, and more intense emissions. In Sicily, mud volcanoes are predominantly found in mountainous areas, such as near Mount Etna, and along the coastal strip, where particularly favorable geothermal conditions result in the presence of gas- and mineral-rich fluids. These phenomena are closely linked to the regional geodynamics, encompassing tectonic and volcanic activity as well as hydrothermal systems. Sicilian mud volcanoes, besides being natural attractions, are studied for their distinctive geochemical characteristics, which partly differ from those in Emilia, especially regarding mud composition and emission temperatures. These features make the mud volcanoes important geological elements with both scientific and touristic relevance (Silvestri, 1866; Etiope et al., 2007; Mammino, 2014; Mazzini and Etiope, 2017).

2. The Salse di Regnano: overview

The Salse di Regnano are located in the Emilia Apennines, specifically in the province of Reggio Emilia, an area that is both geologically fascinating and dynamic. These mud volcanoes lie along the eastern side of the Secchia River valley, a region characterized by mountainous and hilly terrain, intersected by numerous streams that shape the landscape. As previously described, they are geological phenomena caused by the ascent of clayey fluids mixed with gases, primarily methane, originating from deep underground. This ascent generally occurs through fractures or fissures in the Earth's crust, where pressure and temperature promote the separation of organic components and the eventual formation of gases. The result of these processes is the creation of mud cones that erupt to the surface, forming mud deposits of varying sizes (Martinelli and Judd, 2004; Mazzini and Etiope, 2017). In particular, the Salse di Regnano are found in a geologically complex area, characterized by the presence of Quaternary geological units, such as clay and mud deposits, as well as older geological formations. The land hosting these phenomena is the result of a long history of tectonic processes that have shaped the Emilia Apennines, with active and dormant landslides frequently interacting with the mud volcano deposits (De Nardo et al., 2019). In addition to their geological significance, the mud volcanoes of Regnano hold considerable ecological value, as the environment they create serves as a habitat for various species of specialized fauna and flora. Moreover, these areas are often the subject of scientific studies aimed at gaining a deeper understanding of the geochemical and geothermal phenomena that characterize them.

2.1 Some geological evidences

The Salse di Regnano remain active, and their ongoing dynamics are clearly visible not only through the various emission vents but also due to the widespread coverage of the hillside with mud outflows, which show the site's persistent activity. The geological map of the area provides an in-depth view, highlighting not only the mud deposit zones but also numerous sectors characterized by landslides, both active and dormant, and mud accumulations resulting from sliding movements. In particular, the map highlights a variety of these phenomena, enriching the understanding of the morphological and geological complexity of the area.

Figure 1 clearly shows the distribution of all these elements: mud deposits, areas affected by landslide phenomena, both active and dormant, and accumulations due to sliding. In summary, the main identified deposits are as follows: 1) Mud Deposit: composed mainly of pelitic material, with a chaotic structure and, in some areas, lithoid clasts. This deposit is the result of emission cones where mud, saline water, and gases, particularly hydrocarbons, rise from the subsurface; 2) Dormant Complex Landslide Deposit: formed by the combination of two or more types of landslide movements, such as slides accompanied by mud or debris flows. There are no signs of recent movements,

but there is potential for reactivation; 3) Active Landslide Deposit due to Mudflow: originating from the continuous movement of water-saturated mud, behaving as a viscous fluid. Classified as active for direct monitoring purposes; 4) Active complex landslide deposit: a combination of slides and mud or debris flows, clearly active; 5) Dormant mudflow landslide deposit: formed by continuous movement of saturated mud, potentially reactivatable; 6) Active landslide deposit due to sliding: caused by the movement of a mass of earth or rock along a failure surface; 7) Eluvium-colluvium deposit: composed of fine detrital material, such as sands and silts, resulting from in-situ alteration or the combined action of surface runoff and gravity; 8) Dormant landslide deposit due to sliding with potential reactivation: characterized by sliding movements with the potential to be reactivated after long periods of inactivity; 9) Ranzano formation (Val Pessola Member): comprising rocks with alternating layers of lithoid and pelitic material, part of the Epiligurian succession; 10) Ranzano formation (Val Pessola Member): predominantly composed of lithoid rocks, with a high ratio of lithoid to pelitic layers.

An especially interesting aspect is that, despite the active mud volcano area, outlined by the perimeter contours in all the images of the figure, the areas highlighted by the black lines (along with the symbolism shown in the legend) represent the boundaries of the mud deposits. This suggests that the area affected by past phenomena was significantly larger and more active than what is visible today. Disregarding further details and based on the evidence from De Nardo et al. (2019), it is noted that the area to the north of Regnano also features significant and large mud deposits, including those in Casola-Querciola.

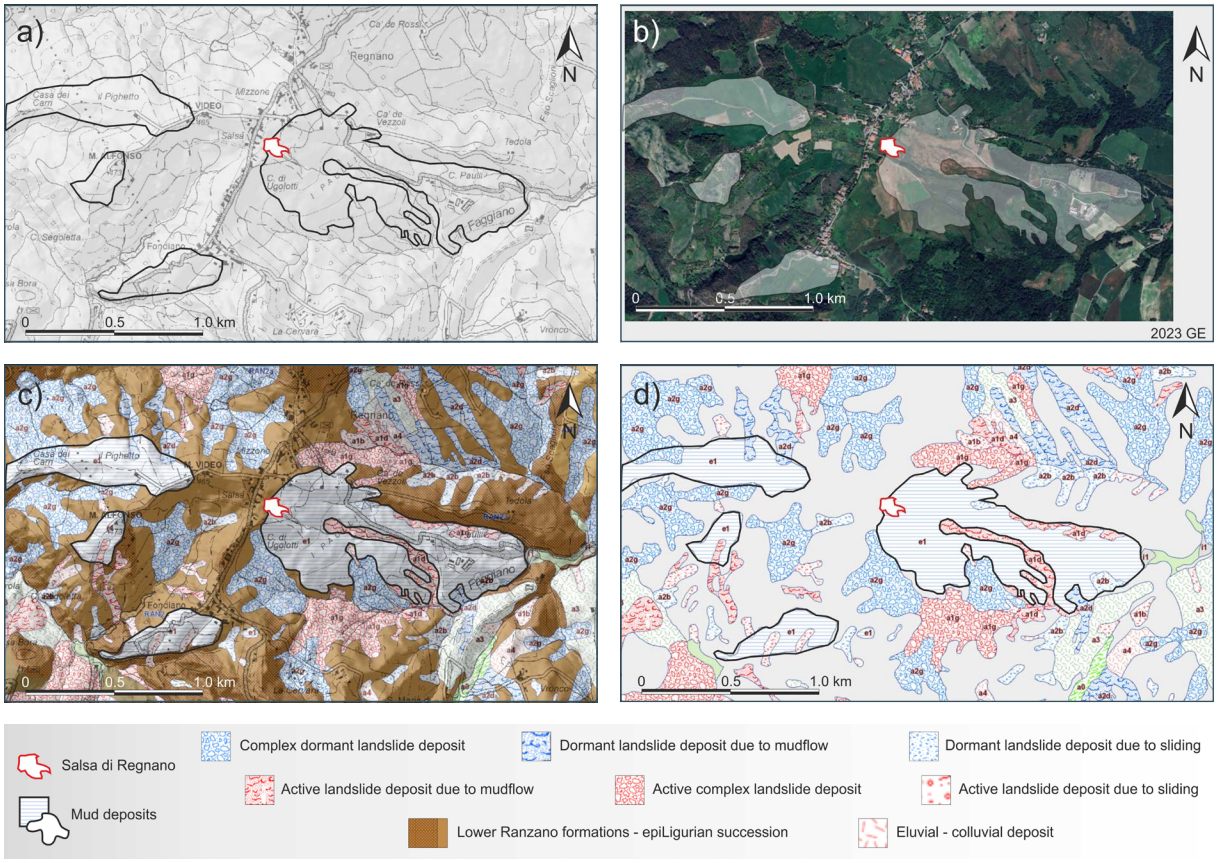

Figure 1. Geological characterization of the area. (a) Regional technical map with altimetric shading; (b) Orthophoto from 2017 representing the same area; (c) Geological map of the area; (d) Map of the Quaternary formations. The boundary of the active mud volcano area (in red) and the mud deposits (in black) is overlaid on each image.

2.2 Some views from space

To better observe the area, it is useful to use satellite (or aerial) images, and in this regard, Google Earth (GE) proves to be particularly valuable due to its free accessibility. It is an interactive platform that lets users explore

high-resolution satellite images and 3D maps of the globe, using data from sources like Landsat, Sentinel, WorldView, TerraSAR-X, and aerial images. The frequency of satellite or aircraft passes varies depending on the mission, and acquisitions can occur weekly or even more frequently depending on commercial needs. However, on GE, image updates typically consist of one or two images per year, depending on the area of interest. Generally, images obtained via aerial photogrammetry tend to have better resolution than satellite images and can be updated more frequently in more urbanized areas. In some previous works (Pesci et al., 2022; Pesci et al., 2024), aimed at assessing the accuracy of terrestrial photogrammetry surveys and the scale of the models obtained, it was possible to confirm that the percentage error on the metrics of images provided by GE is only a few percentage points, values more than acceptable in the comparison between the multitemporal images available on the platform, especially when observing areas of moderate size (less than 1 km).

In the case of the Salse di Regnano, the images available on GE provide an initial reference from 1985, but the resolution is sometimes too low for detailed analysis. Ultimately, the usable images span from 2014 to 2023, offering a limited overview of around 10 years of changes in the area. The time series of images provided by Google Earth highlights the activity of the mud volcano, with the mud flows easily recognizable due to their characteristic grayish color, which stands out sharply in contrast to the surrounding lighter and drier background. This contrast makes the mud emission and deposition phenomena particularly visible. Despite the limitation of annual update frequency, the images allow clear observation of activity episodes, which occur recurrently, but with time intervals of about one year. An interesting aspect is the stability of the mud volcano's boundaries, which remain substantially unchanged over the years, showing how the active zone's boundaries have solidified over time without apparent significant variations, net of weathering erosions. These details confirm the constant dynamics of the phenomenon, despite a relative stability in its extent. Figure 2 illustrates the set of images used, along with the procedure adopted

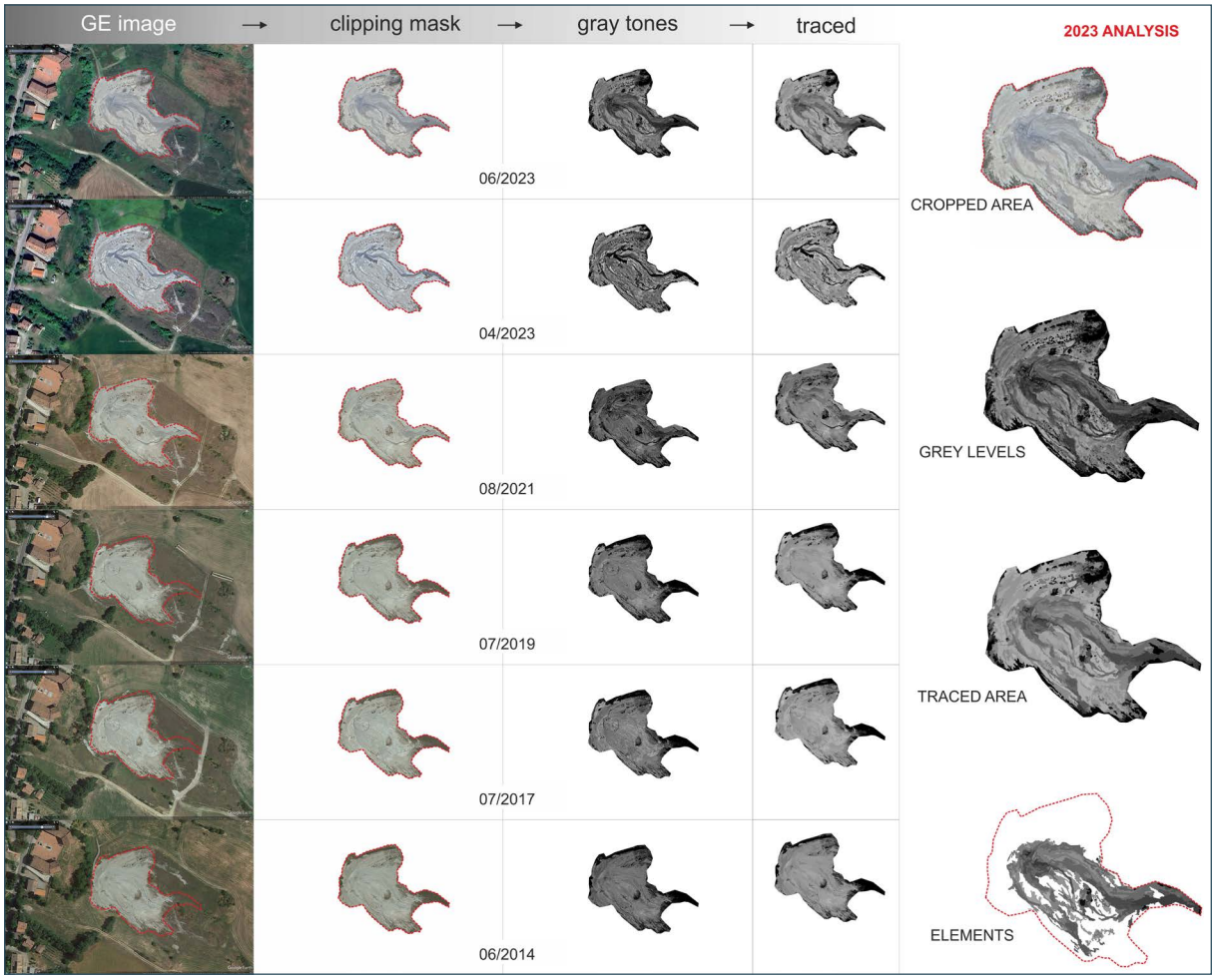

Figure 2. Image analysis procedure from Google Earth. Sequence of operations shown in columns: cropping of the area of interest; optimization and conversion to grayscale; vectorization and extraction of significant elements.

for their optimization and analysis of temporal variations. The processing was carried out using vector graphic software (CorelDraw), through which the images were imported, cropped to areas of interest using a specifically shaped mask, and then converted to grayscale. This color choice, though arbitrary, is motivated by the nature of the material being analyzed. To better highlight the variations, the images underwent a vectorization process using tracing tools, which divide the content into distinct elements, each characterized by a representative average color. This method allows segmenting the image into manageable components, each of which can be individually handled and, if necessary, removed. In the specific case, the light gray elements, corresponding to dry areas not affected by the mudflow, were removed. The final result clearly highlights the geometry of the event, outlining the emission boundaries and the spatial distribution of the material over time, following the path of greatest slope.

2.3 Data from the past

The images used are relatively recent, and even including older photogrammetric images, the maximum temporal extent goes back to the 1980s. It is likely that aerial photographs from the 1950s or earlier exist, but retrieving them and finding those in which the area is clearly visible is a challenging task. Some images available in the regional GIS were reviewed, but the quality is insufficient for detailed analysis, although it was possible to observe the low level of urbanization at the time. To gather historical information, a bibliographic search was conducted starting with De Nardo's (2019) publication, which includes a map created by geologist Biasutti in 1907. Unfortunately,

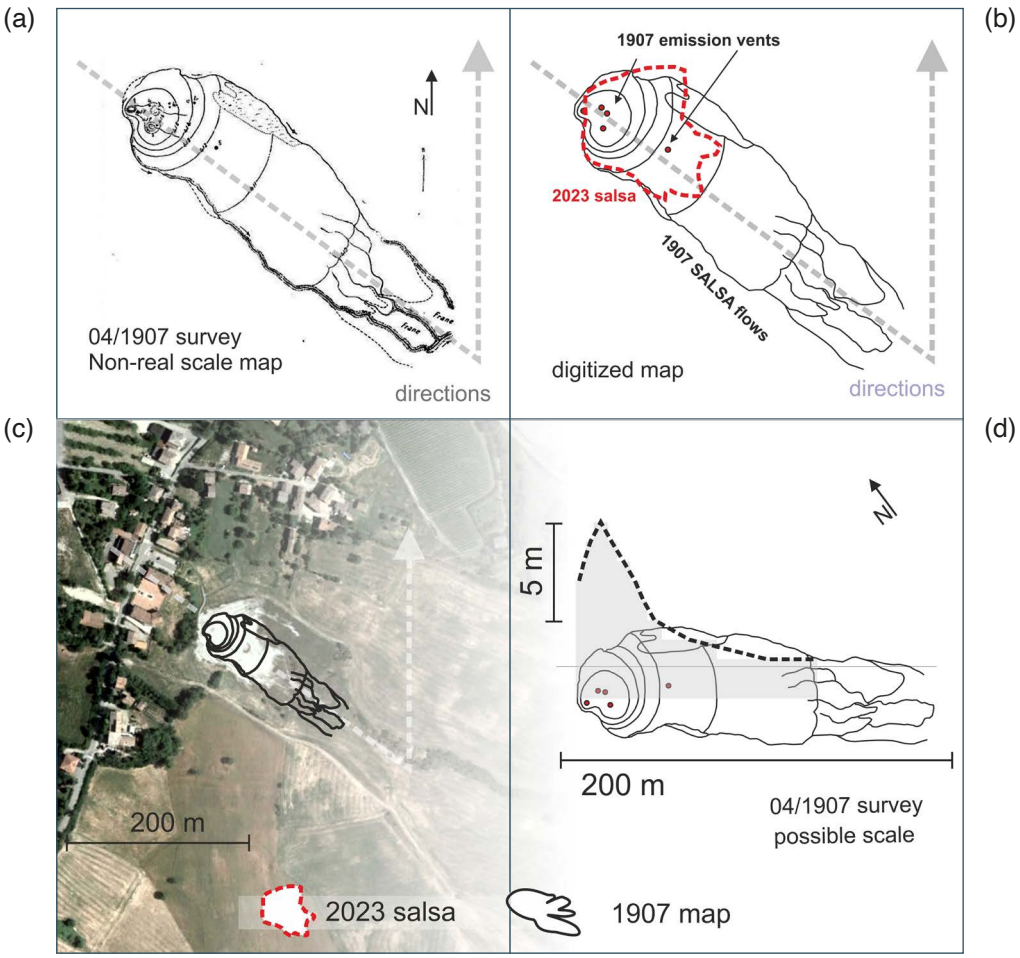

Figure 3. Superimposition of the digitized historical map (a), obtained by digitizing (b) the original document, with arbitrary hypotheses for the localization of the upper part, where the emission vents and well-defined contours are located. Combining historical records with modern datasets yields outcomes that reflect the area's existing appearance (c). In the last panel (d), the profile extracted from the map passing through its central part is shown, with the caveat that the horizontal scale remains only a hypothesis.

the map in the studied paper lacked a horizontal scale, but it was complete with orientation (north arrow) and contour lines (asl) with legible values. Thanks to the availability of the Biblioteca Umanistica at the University of Florence, it was possible to gain direct access to Dainelli's (1907) original paper, which contains a wealth of detailed morphological information, including the length and width of the then salsa area (140 m × 50 m). Additionally, in the general study of the Emilian mud volcanoes, a topographic profile is provided, describing the slope, depression, clay accumulation zones (cones), and distribution along the slope. With this metric information, the map was scaled and digitized using tracing techniques to minimize human error and improve accuracy in feature extraction. The result is a set of polylines and vector elements representing the geometries of the 1907 map, shown in Fig. 3. For the overlay, it was decided (a reasonable albeit arbitrary hypothesis) to consider the main emission zone (vents and mud cones) as stable over time, and therefore the digital model was overlaid onto the current aerial image.

It is important to note that comparing a century-old planimetric model with the current configuration inevitably involves uncertainties. Although the decision to adapt the historical map to the present condition was based on reasoned judgment, it remains partially arbitrary. By also using the altimetric information only and reproducing the vertical profile, a conical structure clearly emerges, corresponding to the main mud volcano (protrusion). This geometry, however, appears significantly different in the current configuration, as will be discussed in the following chapters, with the presentation of photogrammetric surveys.

2.4 Some data from satellite InSar

The European Ground Motion System (EGMS) is an advanced service that provides valuable data to characterize vertical ground variations over time. By using a combination of maps and detailed time series, EGMS allows for highly accurate monitoring of soil deformations. The ability to extract individual time series with a simple click on a scatter plot enables targeted and in-depth analysis of ground dynamics. The system relies on high-resolution satellite data, collected using Synthetic Aperture Radar (SAR) Interferometry technology. Thanks to the use of satellites, it is possible to obtain precise measurements of deformations with spatial resolution that can reach just a few millimeters, making EGMS a reliable tool for monitoring ground changes, even in real time. The data provided by EGMS cover a wide geographical area, including difficult-to-access or remote regions. Recent work by Vradi et al. (2023) validated the EGMS service in terms of spatial coverage and measurement point density across diverse European landscapes, ensuring the accuracy and representativeness of the dataset. This validation supports the confidence in using EGMS data for geological, seismological, and hydrogeological risk studies, particularly in complex areas such as the Emilia Apennines. Here, the data enable precise assessment of ground variations and the risk of subsidence or uplift, phenomena that can significantly influence infrastructure and the environment.

Figure 4a shows the map of vertical ground variations in the Salse di Regnano area. This representation highlights the soil deformations that can be monitored over time using EGMS data. In addition to the time series points, the map includes the boundary lines of the Quaternary coverages, which are essential for understanding the distribution of geological formations and correlating the altimetric variations with the subsurface characteristics. In Fig. 4b, the points are divided into five color categories, each representing a typical behavior of the time series: Red: regular trend with a tendency towards subsidence; Green: phase of lowering followed by a rise; Yellow: similar to green but with more pronounced fluctuations; Light Blue: tendency to descend but with high variability; Blue: very irregular data, with apparent growth. The interpretation of these time series is not always immediate, especially in mountainous areas, where the radar signal can be influenced by poorly identified scatterers, introducing irregularities in the results.

The most reliable scatterers in SAR observations and differential image analyses (InSAR) generally belong to solid and massive building structures or natural elements. These elements are more reliably recognized by the observation system because they are less sensitive to meteorological variations, vegetation cover, and other anthropogenic factors, such as field plowing or other land modifications. As a result, they serve as stable and precise reference points for measuring vertical ground variations. However, even in areas subject to more significant changes, useful data can still be obtained to monitor soil evolution, enabling continuous analysis of deformations over time. In Fig. 4c, some example time series are shown, categorized according to the classification described earlier. The reliability of EGMS data can be influenced by several factors, including systematic errors in vertical calculation and atmospheric interferences. Uncertainties in point positioning, atmospheric variations (such as cloud cover and precipitation),

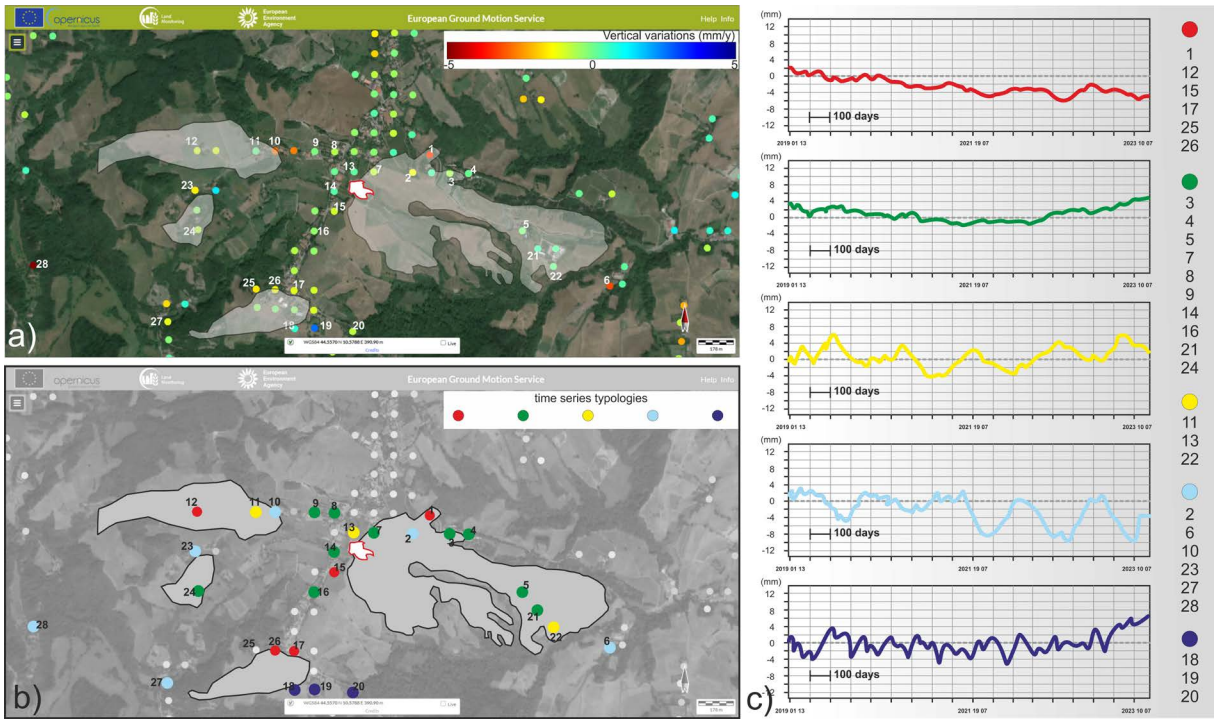

Figure 4. (a) Map of vertical ground variations (velocity), with values ranging from ±5 mm/year. The points represent the scatterers recognized and measured by the system over time. (b) The same map showing selected points classified according to the typical behavior of their time series from 2019 to 2023. (c) Examples of some time series illustrating typical behaviors, alongside the list of displayed points and their corresponding classifications as shown on the maps.

and limitations in spatial resolution can introduce inaccuracies in measurements. Additionally, local geological phenomena can generate non-uniform deformations, making data interpretation more complex. In the specific case of the Salse di Regnano, the study area is very small (less than one square kilometer), which means that atmospheric effects and systematic errors in coordinate determination should be almost uniform across the entire zone. This reduces the risk of significant variations due to these factors, allowing for a more stable and reliable analysis of vertical deformations. In other words, any systematic errors in the calculation of deformations would tend to manifest similarly across all the observed time series. Currently, the data show that the summit area above the active mud volcano region experienced subsidence between 2019 and 2021, followed by uplift between 2021 and 2023, with absolute rates reaching up to about 4 mm per year depending on the yearly trends. A similar trend is also observed in the mud deposit area. However, at this time, the available information is still insufficient to draw solid conclusions about the kinematics of the area.

2.5 Additional notes

According to the CEAS website of the Reggiano territories (https://ceastresinarosecchia.it), the first studies on the Emilian mud volcanoes date back to the 15th century, with the scholar Francesco Ariosto, and later in the 16th century, research conducted by doctors such as Gerolamo Cardano. During this period, the oil present in the mud was believed to have healing properties, promoting its use for medical purposes.

The first significant studies on the Salse di Regnano were carried out between the 17th and 18th centuries. Antonio Vallisneri described them for the first time in 1694, followed by Lazzaro Spallanzani, who carried out further research. In the 19th century, additional investigations were initiated following large eruptions.

In the 18th century, there were paroxysmal eruptions with mud jets reaching treetop height and causing significant ground fissures. During one of these eruptions, the doctor Domenico Gentili ignited the gases emitted by the cones, creating “luminous fountains” that remained visible for nearly two weeks, attracting many spectators. The 19th

century also witnessed important eruptions, such as the one in 1873 when the main cone of the Salse di Regnano reached a height of 7 meters.

In the 20th century, eruptions continued, including one documented in 1930 by Dr. Luigi de Buoi, during which the mud was ejected to a height of 10 meters, and the flow extended 60 meters in length and 90 meters in width. The main crater reached 4 meters in height, and the booms were heard from several kilometers away. This historical information provides a valuable foundation for targeted research aimed at identifying specific references or illustrations to reconstruct the area's past morphology and better understand previous eruptive events. If sufficient detailed data can be gathered, this could enable not only qualitative but also quantitative comparisons with the current state.

3. Photogrammetric Survey of the Salse di Regnano

The remote sensing system used in this study is Structure from Motion (SfM) photogrammetry performed by drone, which involves the use of an Unmanned Aerial System (UAS). An UAS consists of a pilotless aircraft (drone), a ground control station, and, if necessary, other components such as communication systems, sensors, or devices for data collection. At present, UAS are increasingly used for a wide range of applications, including aerial photogrammetry.

3.1 Description of SfM Photogrammetry

Digital photogrammetry based on the Structure-from-Motion (SfM) technique is widely used today in various fields of study and application due to its versatility and relative ease of use. This method is employed in geological surveys carried out from the ground (Pesci et al., 2020; Monego et al., 2020), from aerial platforms (Brunier et al., 2016), or from boats (Pesci et al., 2015). It is also utilized in architectural studies (Teza et al., 2016; Carraro et al., 2019) and for monitoring ground and building deformations (Chen et al., 2021).

One of the main limitations of traditional photogrammetry was the need to accurately know the coordinates and orientation of the camera at the time of acquisition, information that was determined through topographic surveys or provided by the manufacturer in the form of a calibration certificate. The SfM technology overcomes this obstacle through sophisticated algorithms that automatically calculate the internal and external parameters of the cameras, using common points identified in multiple images. This not only enables more flexible surveys but also improves the accuracy and efficiency of data collection, even in complex or hard-to-reach areas. The SfM process typically involves two main stages: image alignment and photogrammetric restitution. The latter associates each pixel with its corresponding position in three-dimensional space, allowing for the creation of a 3D representation of the scene. The first concrete result is a point cloud, which is a set of spatial coordinates (x, y, z) enriched with RGB color information. To obtain a realistic and correctly scaled model, a scale factor must be introduced, which can be defined using a network of Ground Control Points (GCPs) (Brunier et al., 2016) or through direct georeferencing in drone surveys equipped with GNSS systems and inertial platforms (Turner et al., 2014). Some advanced software allows the application of the scale factor in post-processing (Pesci et al., 2016).

Surveys performed with lightweight drones often rely on images captured with compact digital cameras, whose small sensors can limit data quality compared to professional cameras. However, lightweight drones offer significant logistical advantages, enabling surveys in areas that are difficult to access. To obtain accurate data, it is crucial to ensure a high overlap of images and a uniform distribution of viewpoints. In drone surveys, the flight often follows a serpentine path to maximize the quality of the data acquired. SfM technology enables the creation of detailed three-dimensional models through a combination of close-range digital photogrammetry, computer vision techniques, and the high computational power of modern workstations. Metashape software (formerly Photoscan, Agisoft, 2021) performs image matching through advanced algorithms, likely based on principles similar to the Scale-Invariant Feature Transform (SIFT) method (Lowe, 1999), with proprietary enhancements. The software also uses bundle adjustment (BA) techniques to refine the reconstruction of the three-dimensional coordinates and the camera positions.

An additional advantage of SfM modeling is its compatibility with a wide range of cameras, including consumer models, as long as adequate image overlap is ensured. The best results are obtained with full-frame cameras, thanks

to their large sensors that improve image quality by reducing noise and increasing spatial resolution. Smaller sensors, such as those installed on ultralight drones, can introduce limitations in modeling, especially if the image overlap is insufficient.

The role of SfM photogrammetry is particularly valuable in complex environments such as the Salse di Regnano, where high-precision data is required. In high-precision surveys, the choice of equipment is crucial to ensure accurate results. The use of full-frame cameras, paired with high-quality lenses, helps to reduce errors such as the rolling shutter effect and ensures reliable calibration. These aspects are essential for high-resolution photogrammetry, especially in geologically complex regions (Westoby et al., 2012; Pesci et al., 2020; Pesci et al., 2022).

3.2 Survey Settings

The photogrammetric survey of the Salse di Regnano was conducted on February 20, 2025, using a Matrice 350 drone equipped with a ZenMuse P1 full-frame camera and an RTK system for precision positioning. The camera, specifically designed for aerial surveys, features a focal length of 35 mm, ensuring the high geometric precision required for detailed photogrammetric analysis and an accurate representation of the landscape (de Lima et al., 2021). Two of the flights conducted were analyzed and used to create photo-realistic digital models: the first to provide a detailed and confined representation of the active mud volcano area, and the second to extend the study area, creating a geometrical reference context.

The first flight was carried out at an altitude of approximately 120 m (AGL), acquiring 135 images along a meticulously planned flight path. This path was designed to ensure at least a 70% overlap between consecutive images, both longitudinally and transversally. The total surveyed area was about 0.13 km^2, covering nearly twice the area affected by the mud volcanoes, landslides, and material accumulations. In this configuration, the ground resolution was 1.4 cm/pix (GSD).

The second flight aimed to expand the study area towards the adjacent fields on the slope below the town. At an altitude of 120 m (AGL), 216 images were acquired along a path that followed horizontal and longitudinal lines, covering about 0.15 km^2. To reduce data load during the analysis phases, the image overlap was reduced. It is important to note that flight strategies were constrained by regulatory limitations, and in this specific case, it was not possible to increase the flight altitude. To extend the observation, a lower overlap was therefore chosen. The flight path was continuously corrected in real-time using Real-Time Kinematic (RTK) positioning applied to the data provided by a GNSS receiver, ensuring precise georeferencing throughout the survey. Spatial positioning corrections were transmitted via Wi-Fi and mobile networks, achieving a horizontal accuracy of less than 2 cm and a vertical accuracy of less than 3 cm. These corrections significantly improved the data acquisition precision, allowing for a detailed analysis of surface ground deformations. Detailed information related to the camera, drone, survey

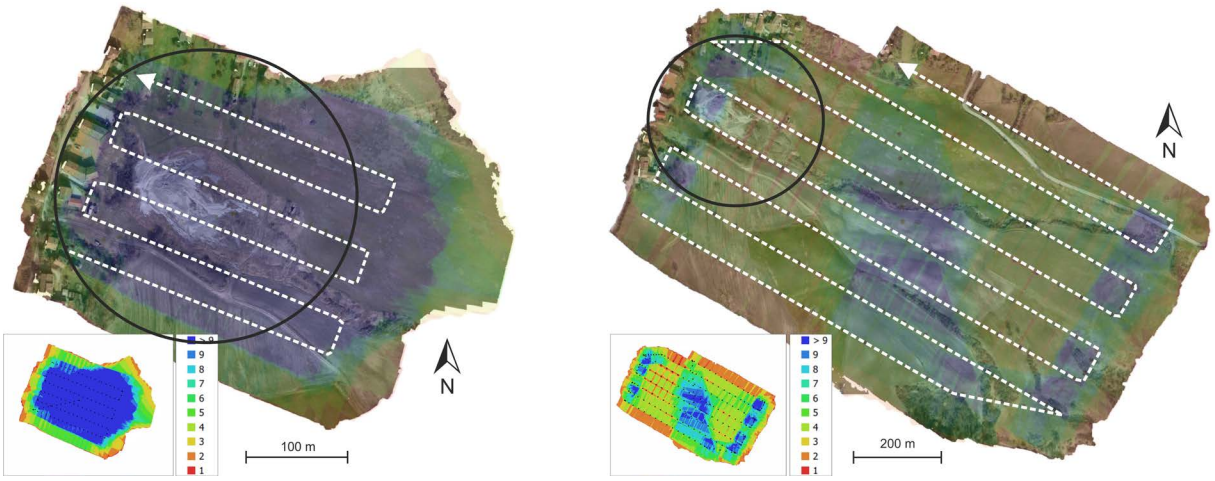

Figure 5. Flight 1 and Flight 2. Map of the overlays in transparency on the SfM model, with the drone's path and the area of the active mud volcano highlighted within the circle. At the bottom, a map with a full-color legend illustrating the survey and coverage areas.

Table 1. Technical Specifications, Flight Settings, and Main Products of SfM Analysis.

UAS	Parametes	Flight/Analysis	Parameters Volo 1	Parameters Volo 2
Camera	DJI Zenmuse P1	Images number	135	216
Focal length	35 mm	Flying altitude	120 m	120 m
Aperture	f/2.8-f/16	GSD	1.4 cm/pix	1.4 cm/pix
Sensor size	8192 × 5460 px^2	Coverage Area	0.13 km^2	0.15 km^2
Sensor size	35.9 × 24 mm^2	Tie points	81.3K	284.5K
UAV	Matrice 350 RTK	Cameras	135	216
Weight	6.47 kg	Coordinate System	WGS84	WGS84
Battery	TB65	Point cloud points	38.4M	143.1M
Max speed (m/s)	23 (~80 km/h)	Texture size	4K	
Max Flight time	55 min	Model resolution	22 cm/pix	27 cm/pix
Navigation Systems	GNSS	Orthomosaic size	32.9K × 27.8K	68.9K × 51.8K
RTK accuracy H	1 cm + 1 ppm	Tie points	81.3K	284.5K
RTK accuracy V	1.5 cm + 1 ppm	Processing time	1.1 h	1.3 h

parameters, and data processing methods using Metashape software (www.agisoft.com) are summarized in Table 1. This table, which plays a crucial role in the final analysis of the photogrammetric data, will be referenced later to describe the various phases of the analysis. The choice to include both the UAS system technical specifications and the characteristics of the models obtained through SfM analysis in one section was intentional, to provide a complete and concise overview of the adopted methodologies.

The above description is illustrated in Fig. 5, where the survey data are presented through a series of information layers: the point cloud at the bottom, the image overlap map (shown in false colors) in transparency, and the drone flight path for both flights. The ability to obtain 3D point clouds and textured models, enriched with the colors of the acquired images, allows for the analysis of the surveyed area both geometrically and visually. This approach provides a representation of the area that simulates the experience of an operator walking on the mud volcano and the flows, closely observing its features. It is possible to recognize various components, such as the emission vents, the flow areas, and the traces left by the flows, effectively capturing these phenomena over time while also measuring them precisely, as will be illustrated in the following sections.

3.3 Point Cloud Management and Post-Processing

The primary outcome of the SfM analysis is the transformation of a set of images acquired by a drone into a georeferenced three-dimensional point cloud. In the specific case of a UAS system equipped with RTK technology, the images are enhanced with high-precision metadata, improving the quality of spatial reconstruction and reducing positioning errors. After the generation of the point cloud, post-processing involves several essential operations for

model analysis and visualization. The initial point cloud, which assigns precise spatial coordinates to each point along with color information derived from the photographs, represents the raw dataset from which subsequent processing steps are derived. The main phases of point cloud management include:

1) Creation of the 3D Triangulated Model: The point cloud is processed to generate a 3D mesh, i.e., a continuous surface obtained through the triangulation of points. This step transforms the model from a scattered set of coordinates into a solid structure, which can be used for geometric, volumetric, and deformation analysis over time. However, during the conversion from point cloud to triangulated model, some details are lost, as the interpolation process reduces the density of spatial information.
2) Creation of Texture and Orthophoto Mosaics: Once the triangulated mesh is obtained, a "textured cloak," i.e., a mosaic of the original images adapted to the geometry of the model, can be applied. This step allows for a visually detailed representation of the scene, combining the geometric precision of the 3D model with the quality and realism of high-resolution images. Texturing is particularly useful for applications where visual appearance plays a crucial role, such as monitoring geologically active areas, architectural restoration, or analyzing natural surfaces.
3) The combined approach of point cloud and textured model offers a balance between precision and usability: the point cloud retains the maximum density of spatial data, while the triangulated model, despite a reduction in geometric accuracy, allows for navigation within the surveyed space with a high level of visual detail. Thanks to this method, the SfM analysis not only provides highly informative 3D models but also allows for the realistic exploration of territorial features through an immersive and detailed reconstruction.

3.4 Preliminary Analyses

In addition to the preliminary visual and geometric inspections, which help identify the areas of interest and measure their position and size, the main analysis described in this work focuses on the most appropriate method for observing the detailed morphology of the area. The objective is to select the most suitable representation for extracting information about the arrangement and configuration of the mud volcano, surpassing the informational limitations of the basic altimetric model. Specifically, the approach used by Pesci et al. (2016) involves the creation of reference primitives and the calculation of the point-to-plane distance, represented using custom color scales. The results obtained, based on different choices related to the primitives, carry a technical significance that depends on the type of primitive selected. For example, if the primitive is a horizontal plane passing through the lowest point of the model, the map will represent altimetry relative to an arbitrary origin. If the primitive is a fit plane, calculated using a least squares approach with all the points in the model, the map will represent the deviation from the average position of the points. If the plane is defined using the boundary contours of the area of interest, the map will represent the arrangement of points relative to the external environment.

In general, the most commonly used primitives in slope studies are planes or sets of planes, as these are the most indicative parameters for characterizing the morphology under examination, such as in the case of a slope modeled by a plane or an area of the slope represented by a fan of planes. In summary, the importance of a physically meaningful reference element lies in its role as a reference for observing the surveyed area, allowing for a quantitative and functional characterization of the morphology.

In the case study presented, several reference planes were adopted. A horizontal plane, raised to touch the lowest point of the model, was used as the base for relative altimetry. Additionally, fit planes were considered, obtained by interpolating specific selections of points or the entire point cloud, to create a representative reference for the area under examination, with a clear and well-defined physical meaning. In Fig. 6 (a and b), the larger model from the second flight is shown, along with its altimetry. This altimetry represents the distance between each point of the model and a horizontal plane passing through the lowest point of the scene. The height ranges from 0 to 140 meters over about 1 km. It's important to note that, at this scale, the buildings at the top of the slope are not visible because their roofs are too small compared to the model. As we move upwards, the height differences are gradual, and the area looks like an inclined plane of about 14°, oriented east-southeast. The highest part of the model shows a pattern that seems different from the surrounding area. Here, the terrain flattens out slightly with a small fissure, suggesting a step-like feature, and a more depressed area. This could indicate a landscape change that might have an anthropogenic influence. To better understand the area's morphology, a fit plane was calculated using subsets of the point cloud. This choice was made to simplify the analysis. In Fig. 6 (c and d), the interpolated

plane and its position in space are shown, highlighting areas above and below it. The colors of the point-to-plane difference map clearly identify the mud areas as depressions between surrounding hills. Some areas with positive values appear lower down the slope, suggesting possible accumulation zones or landslide deposits.

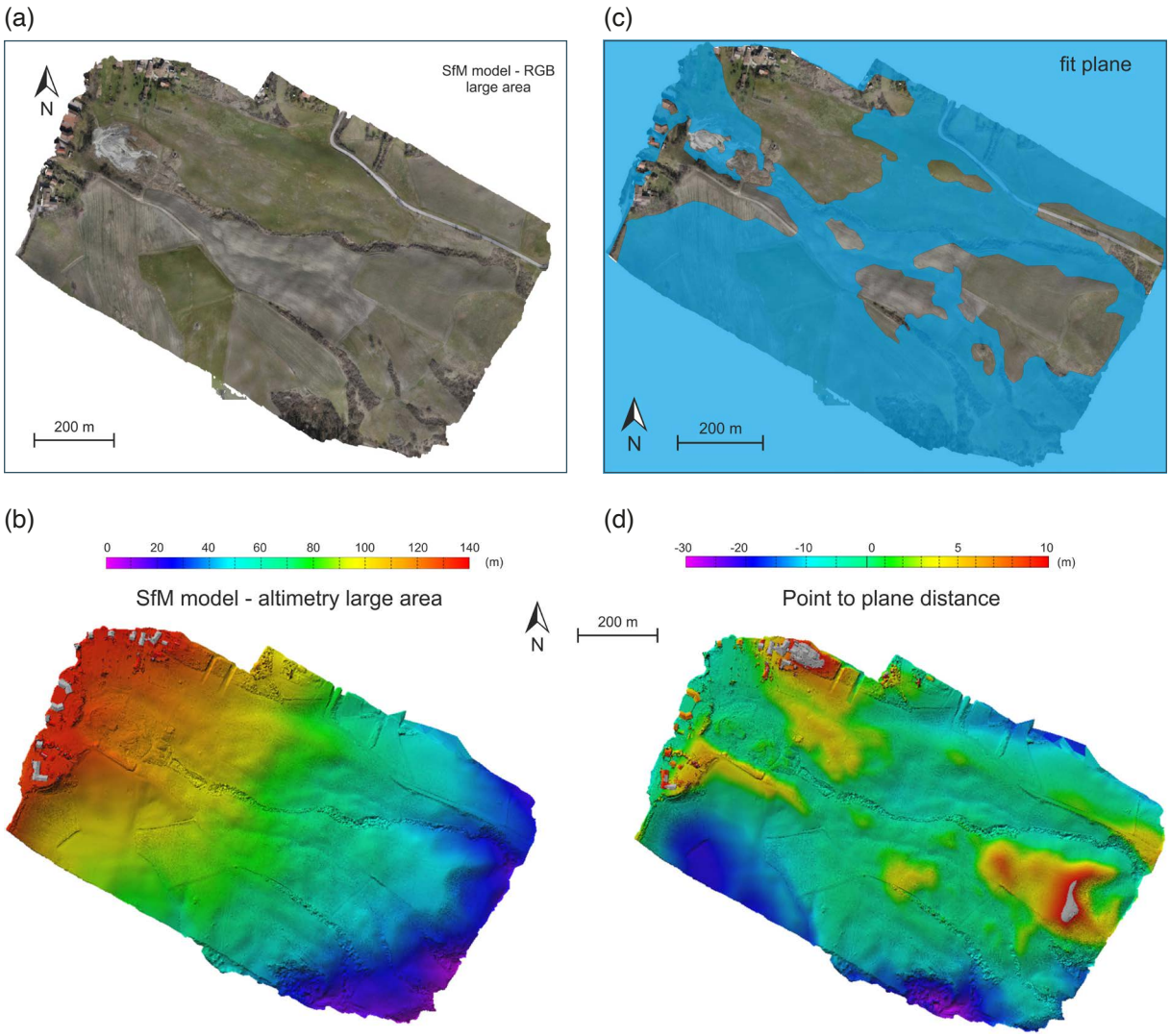

Figure 6. (a) SfM model from flight 2, showing the active mud area and surrounding zones over an area of approximately 800 m × 600 m. (b) Relative elevation, with a scale ranging from 0 to 140 m. (c) Fit plane. (d) Corresponding difference map.

For a more detailed analysis, the same procedure was applied to the point cloud derived from flight 1, providing a more precise survey of the active mud area and the immediately underlying zones. The results are in Fig. 7: a point-to-plane map was created using a fit plane, which interpolates the points from the mud area (excluding zones with very steep relief); finally, a point-to-plane difference map was generated using a plane interpolated from the points representing the higher areas above and around the mud.

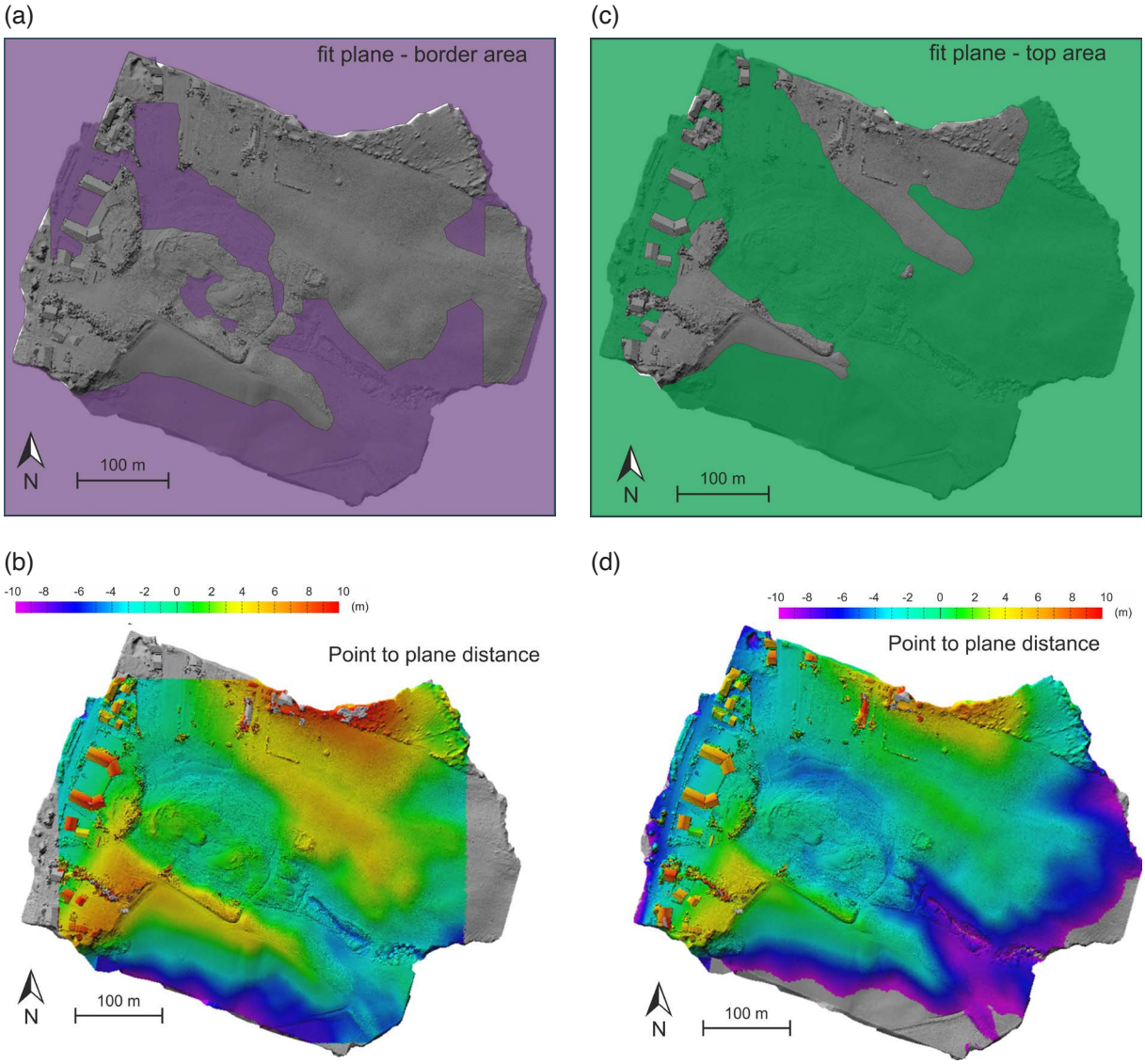

Figure 7. (a) The fit plane representing the mud area, interpolated using all points except those on the steeper reliefs, to highlight the layout of the area of interest in the most useful way. (b) Corresponding point-to-plane map. (c) The fit plane representing the higher areas compared to the underlying slope zones. This figure is similar to the previous one, but with more pronounced discontinuities and a more visible terrain depression. (d) Corresponding map.

3.5 Cross sections

To better analyze the area's morphology, cross sections were generated to visualize elevation changes across different transverse profiles. These sections, derived from the previously defined fit planes, effectively illustrate the elevation variations along the area's profile. This visual representation enhances the understanding of local topography and complements the insights gained from the morphological maps (Fig. 8). The analysis of the cross-sections immediately highlights that the sections outside the mud area context exhibit a distinctly regular pattern. The first section (y = 100 m) shows a relatively modest elevation up to 50 meters along X, followed by a gradual descent with a slope of about 10 meters over 150 meters of distance (about 4°). This behavior suggests a relatively uniform morphology before the onset of phenomena that may have influenced the slope profile. The second and third sections (y = 160 m and y = 180 m), on the other hand, highlight a clear discontinuity in the profile, indicating the presence of a significant step at the mud area. In these sections, the descent is characterized by an average slope of about 50 meters over 350 meters (about 8°), but it is interrupted by irregular formations

and more unstable segments, due to accumulations and landslides present on the slope, largely covered by clayey material. This type of morphology suggests the activity of land instability processes, which have shaped the surface in a discontinuous and irregular manner. The fourth section, located beyond the mud area, presents a more regular geometry and a gentler slope, free of obvious discontinuities in the upper parts, suggesting greater slope stability in this area. Furthermore, the sections crossing the active mud area lie significantly lower than the external ones, suggesting a depression typical of the landslide zone. This feature may result from collapse or progressive erosion, helping to define the geomorphological behavior of the slope.

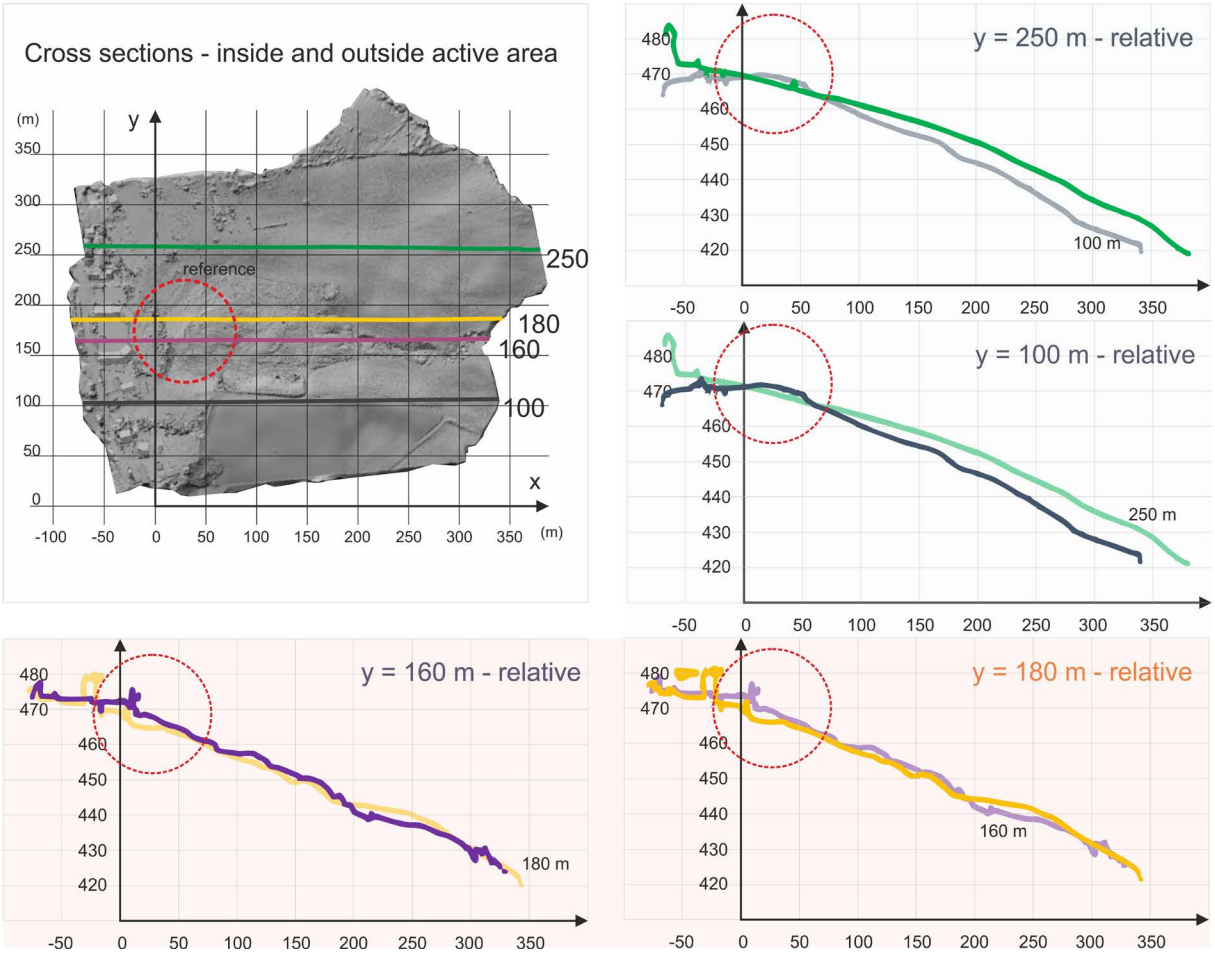

Figure 8. Four cross-sections were extracted from the 3D model by intersecting it with vertical planes, using a rotated reference system aligned with the main slope direction (X-axis), obtained by counterclockwise rotation from the vertical axis, to facilitate visualization. Two sections (in purple and yellow) intersect the inner part of the mud area (at Y = 160 and Y = 180), while the other two (in black and green) are external to the emission and landslide zone, located in undepressed areas. The graphs display the profiles with transparency to highlight the morphological variability within and outside the active zone, balancing clarity and visual simplicity through an arbitrary design choice.

Summarizing the observations derived from the previously presented analyses, we can list the following findings: 1) The mud area appears to be confined within a ground depression; 2) The area occupies approximately 15×10^3 m^2 and shows evident morphological changes due to deposits and accumulations of extruded material; 3) Small emission vents are observed near a nearly flat crater, from which, in the current configuration of the mud, the main flow propagates; 4) Both the active area and the underlying zone are bounded by portions of the slope that are higher and more regular; 5) In the lower part of the area, moving downward, clayey masses with blunt and rounded shapes are observed; 6) The upper area, near the buildings, is elevated relative to the elevation levels of the upper part of the mud, showing a well-defined vertical discontinuity in relation to the mud area.

3.6 Visual inspection and comparison

In addition to the morphological analyses previously described, some images derived from navigating within the textured models are presented (Fig. 9). These images were selected to provide a visual complement to the false-color maps, allowing a more detailed and three-dimensional observation of the area's morphology, as well as the structural features identified during the analysis.

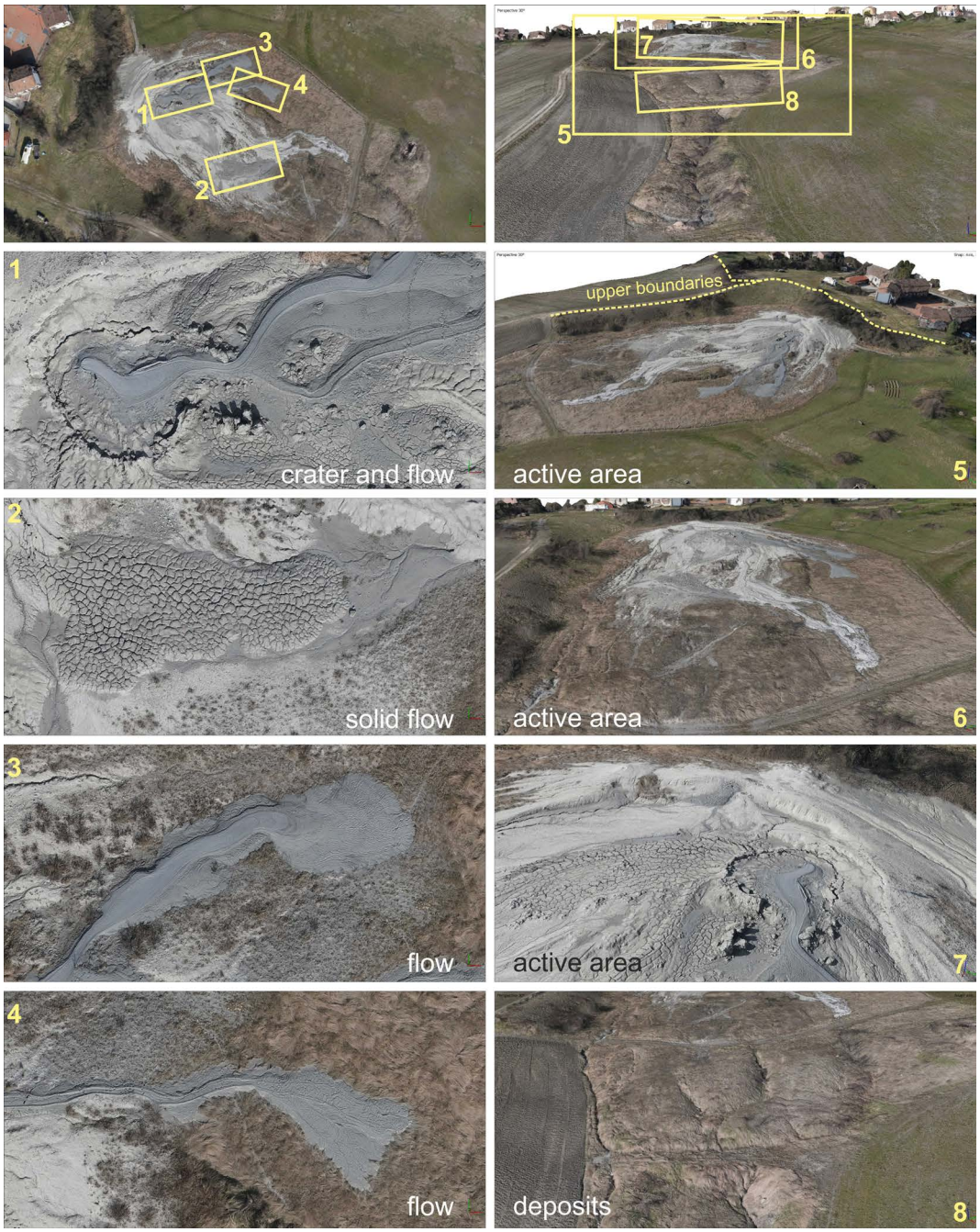

Figure 9. Textured mesh derived from the analysis of flight 1 images. On the left, top-down views are shown, and on the right, perspective views within the model. The 8 boxes, cumulatively indicated in the upper images, are subsequently enlarged and numbered in the rows below. (1) Most active vent with mud flows and the surrounding crater area; (2) Detail of a solidified flow; (3) Recent and still fresh flow; (4) Second branch of the most recent flow; (5) Overall view of the mud area, including the summit zone near the buildings, with evidence of a topographic discontinuity; (6) Enlargement focused on the mud area; (7) Further zoom to highlight the emission vents; (8) Lower part of the active zone with material accumulations.

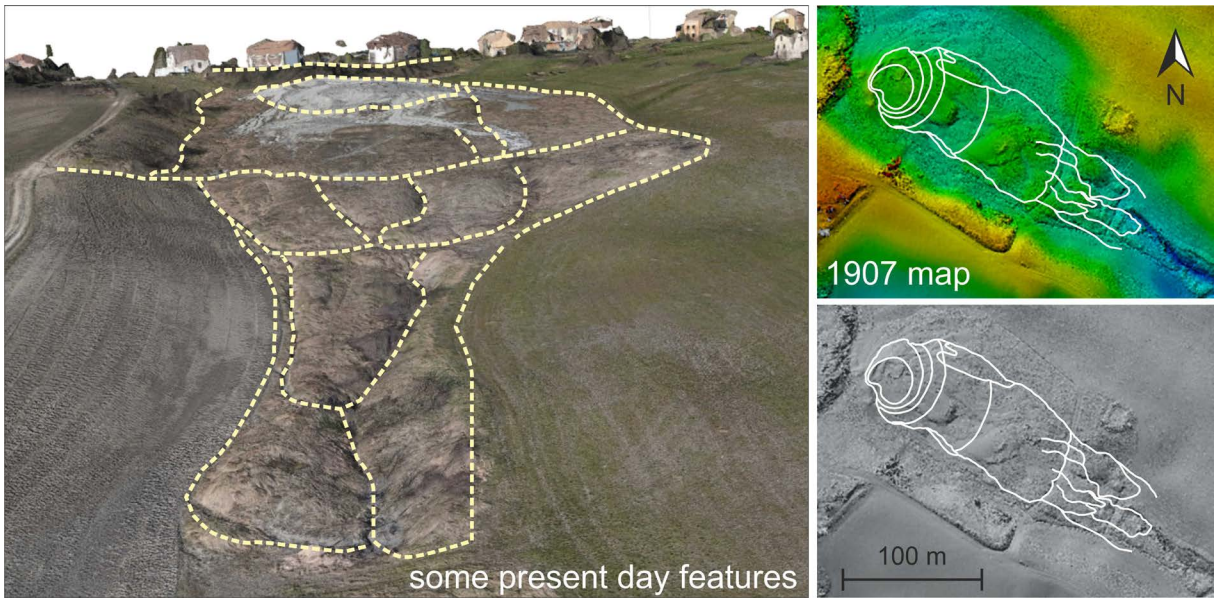

Figure 10. The main present-day features observed in the area (dashed lines) alongside the historical contours from 1907. The old data is overlaid onto the morphological and geometrical map (shown in the right panels). Note: The size of the 1907 area is inferred from historical text, and its positioning on the recent model is a hypothesis (highly probable, but still a hypothesis).

Moreover, Fig. 10 highlights some key features outlined in a frontal view of the area. To facilitate a visual comparison between the present and the past, the contours from the old map are overlaid onto the digital models, providing a clearer understanding of the changes over time.

The main features observed in the textured models are shown here, with the 1907 map overlaid and adjusted for scale and orientation. As previously mentioned, the proposed hypothesis is based on contour lines and certain accumulation patterns that closely resemble those depicted in the 1907 map. This visual similarity suggests a possible correlation, though further analysis is needed to confirm it. Supporting this interpretation, Fig. 11 presents the original 1907 slope profile, which includes the mud area. However, uncertainties remain regarding the accuracy of the image, the scale, both horizontal and vertical, and the viewing direction, which is not explicitly stated. Was the cross-section drawn along the main slope, or from a different viewpoint? Since this cannot be determined with

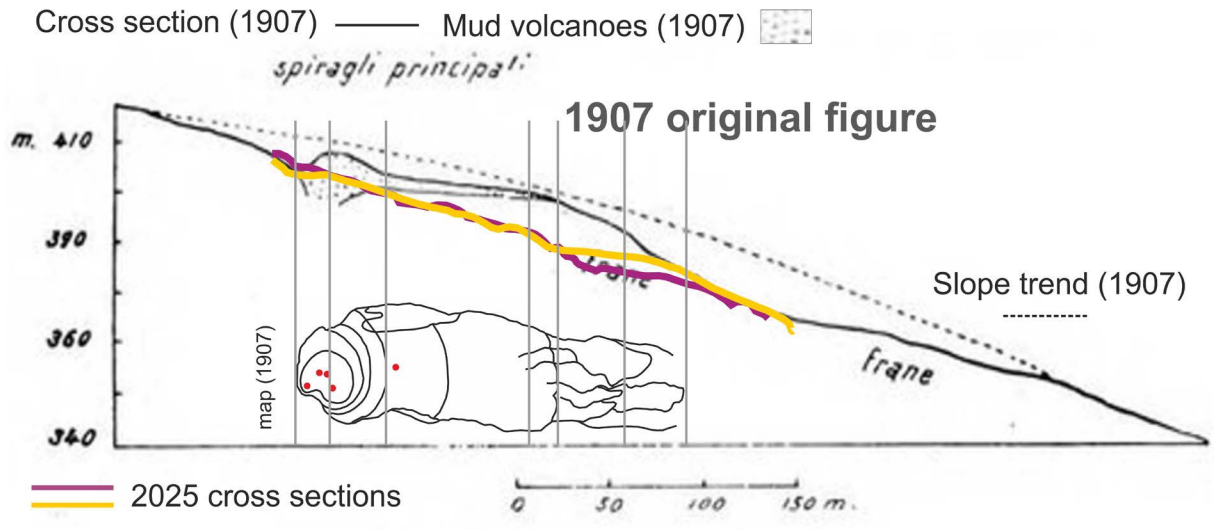

Figure 11. Graphs of the profile of the ancient and current area (1907-2025). Below, the map of the area scaled according to the information provided in Dainelli (1907).

certainty, some ambiguity persists. Nevertheless, a comparison with modern sections is still possible. Figure 11 shows a direct comparison between the historical and current profiles, using two extracted sections. Despite the uncertainties, a clear change is visible: in the upper area, where a tall system of mud cones once stood, the surface is now significantly lower. It is likely that the accumulated material along the central body of the area, possibly including the landslide mass, has collapsed, reshaping the overall profile. The 1907 model has also been inserted, rotated and scaled to match the current profile, showing a remarkably good fit with the observed discontinuities.

The results shown in this section clearly highlight a significant change in the landscape, despite the uncertainties and possible inaccuracies in the historical data. Through the comparison of vertical cross-sections and early 20th-century topographic sources, it becomes evident how the morphology of the Salse di Regnano area has evolved over time.

4. Geochemical Measurements of Fluids

The gases emitted by Italian mud volcanoes are predominantly composed of methane, typically exhibiting carbon isotopic ratios lower than −30‰, which suggest a mixed origin from both biogenic and thermogenic sources. The detection of ethane further supports the presence of a thermogenic component, indicating that gas emissions in these areas result from the interplay between biological activity and deep geological processes (Martinelli and Judd, 2004). This dual origin provides key insights into the complex fluid migration pathways and subsurface dynamics, including the identification of tectonic features or preferential degassing zones. However, the classification of gases as strictly biogenic or thermogenic, based solely on δ^{13}C-CH_4 values or the presence of minor hydrocarbon species such as ethane, remains an area of debate. In many cases, δ^{13}C-CH_4 signatures attributed to biogenic processes can also arise from secondary microbial alteration of deeper, thermogenic methane. Furthermore, mixing processes, microbial oxidation, and interactions with host sediments can blur the isotopic distinction between sources. This ambiguity is particularly relevant in cold mud volcanoes of the northern Apennines, where surface conditions favor microbial activity, but deeper contributions from thermogenic or abiotic sources may still be present. As such, caution is needed when interpreting geochemical signals, and additional tracers (e.g. δD-CH_4, noble gases, or molecular ratios) may be required for more robust source identification.

Gas flux measurements, particularly in diffusive degassing areas, are commonly conducted using the "accumulation chamber" technique (Chiodini et al., 1995). This method involves placing a chamber on the soil surface, equipped with an internal fan to promote air circulation. A pump then extracts air from the chamber for analysis using external gas sensors – an infrared spectrometer for CO_2 and a tunable laser diode spectrometer for CH_4. The system detects changes in gas concentrations over time, which are subsequently converted into flux rates (e.g. $mol \cdot m^{-2} \cdot d^{-1}$ or $g \cdot m^{-2} \cdot d^{-1}$) using calibration parameters that depend on the chamber's geometry and ambient environmental conditions.

At the Salse di Regnano, the emitted gases are primarily methane (CH_4), accounting for 97.4% of the total concentration, with a carbon isotopic signature of −44.9‰, pointing to a predominantly thermogenic origin. CO_2 is present at 1.14% and ethane (C_2H_6) at 0.72% (Minissale et al., 2000). The active vents exhibit low and intermittent degassing activity, with bubbling occurring every few seconds, suggesting a stable and modest emission regime.

To explore gas flux distribution, a diffusive soil gas survey was carried out on 20 February 2025. Fluxes were measured across 51 grid points spaced ~14 meters apart. CO_2 fluxes were detected at all sites, while measurable methane emissions were found at only seven points, indicating a heterogeneous gas distribution. Due to this disparity, interpolation focused solely on CO_2 data, using a sequential Gaussian simulation algorithm (Cardellini et al., 2003).

The spatial pattern of CO_2 fluxes reveals elevated values around the mud deposits, likely due to biogenic CO_2 production in the soil, while emissions directly above the mud vents are lower, consistent with the low activity observed. Total CO_2 output is estimated at 0.13 ± 0.01 tons per day.

Methane emissions show a more localized distribution, occurring near active mud vents, particularly in areas with exposed mud, surface cracks, or fractures, which act as preferential pathways for gas escape. However, due to their limited occurrence and high spatial variability, methane fluxes could not be interpolated, and total emissions remain unconstrained. Still, based on the observed magnitudes, the overall methane flux at Regnano appears low, especially when compared to more active sites such as the Salse di Nirano (Sciarra et al., 2017).

These preliminary geochemical data offer a first glimpse into the fluid dynamics at Regnano. While the results highlight clear spatial trends in CO_2 and methane emissions, further investigations are needed to better understand

the controlling processes and the broader environmental significance of the gas fluxes. In particular, more refined geochemical tools and extended isotopic datasets could help clarify the relative contributions of biogenic and thermogenic sources in cold mud volcano settings such as Regnano.

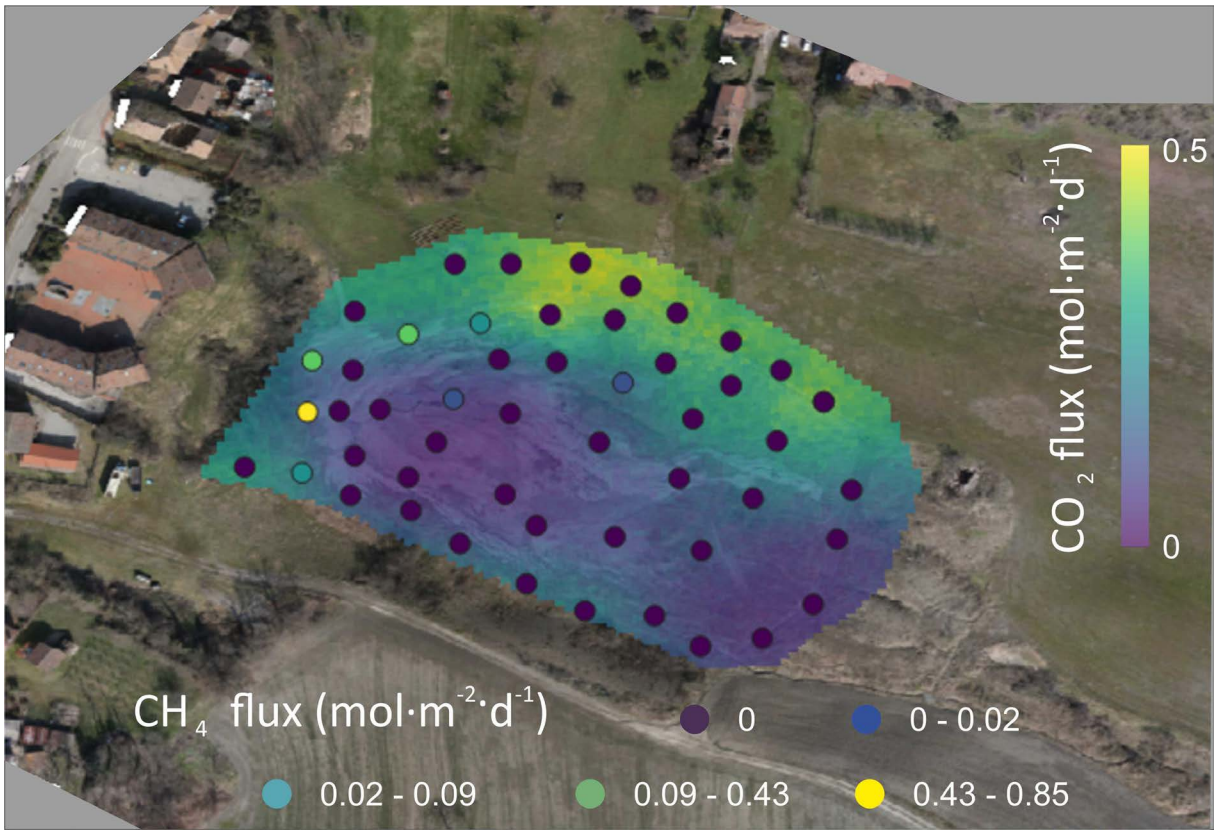

Figure 12. Geochemical surveys of methane and CO_2. Measurements were taken at approximately 50 points distributed within and near the active area. The CO_2 data highlight significant values on the right side of the area (north), with daily fluxes reaching 0.5 $mol \cdot m^{-2} \cdot d^{-1}$. Methane measurements also show similar maximum values, but mapped at specific points within the emission area, not observed elsewhere.

5. Preliminary conclusions and future work

The data gathered through photogrammetric surveys, gas measurements, and morphological analyses provide a detailed overview of the Salse di Regnano, highlighting the need for further investigation into the ongoing geological processes. Geological maps indicate that the active area is part of a larger depositional system extending south and west of the town, with significant deposits also present in the nearby Querciola area. These findings suggest a history of notable extrusion and eruption events shaping the lower Apennines landscape.

Satellite observations over the past two decades show little change in the configuration of the active area. However, the 1907 historical map suggests a gentler slope and a more pronounced elevation at the summit of the vents, typical of mud volcanoes, potentially indicating a collapse or partial filling of the area over time. Due to the lack of a precise horizontal scale in the historical data, this hypothesis will need to be confirmed by more in-depth studies of the historical relationship, but even now, a clear difference in shapes can be observed in the emissive areas.

Kinematic analysis based on satellite interferometric data (EGMS) reveals temporal trends that are not clearly correlated with the geological units, indicating that further research is necessary to better understand the area's dynamics. Cyclical variations and inverse trends observed in recent years highlight the complexity of the system, suggesting that simple annual averages of vertical movements may not fully capture the underlying processes.

Photogrammetric and morphological analyses suggest that the Regnano mud volcanoes may have experienced a collapse, possibly in the early 20th century or earlier. The area is characterized by a slope degrading toward the

east-southeast, with active vents, flows, and accumulations indicating a typical clay slide scenario. The surrounding terrain is higher, implying that landsliding may have contributed to lowering the soil compared to its original morphology.

Although limited by the absence of a precise horizontal scale, the historical map analysis allows valuable comparisons between past and present morphologies. The 1907 profile, though not directly comparable to the current situation, suggests significant morphological changes, possibly related to a major geological event such as the landslides and collapses documented around 1930.

Geochemical surveys revealed methane (CH_4) and carbon dioxide (CO_2) emissions, with significant CH_4 values detected near the vents, especially where fractures facilitate gas escape. Integration of these findings with satellite imagery and spatial analyses has enabled the development of a methodological framework to guide future investigations, including the planning of geomagnetic and passive seismic surveys aimed at better characterizing the subsoil. These efforts should also encompass targeted sampling and analysis of bituminous and oily liquids observed in the field, which may provide additional geochemical evidence of deep-sourced thermogenic hydrocarbons associated with mud volcano activity.

Finally, while the preliminary data offer valuable insights into the ongoing dynamics of the Regnano mud volcanoes, further research is essential to fully comprehend the area's geological evolution. The integration of advanced geophysical techniques will be key to refining our understanding of subsurface processes and their impact on the landscape. This approach appears to be an effective tool for guiding subsequent investigations, providing a structured framework for future studies.

Acknowledgements. The authors wish to thank Paola Cusano, project manager of PROMUD, part of the Pianeta Dinamico program supported by INGV, for the opportunity to conduct this research within the WP2 operational unit and for her continuous support. Thanks to Cecilia Ciatti and to the "Biblioteca Umanistica" of the University of Florence for their support in the bibliographic research

References

Biasutti, R. (1907). Materiali per lo studio delle salse – Le salse dell'Appennino Settentrionale, Memorie Geografiche, Suppl. Rivista Geografica Italiana, Giotto Dainelli, 2, 101-255.

Bonaposta, F., L. De Nardo, F. Govi and G. Ferrari (2018). Geologia e geodinamica delle salse di fango dell'Appennino Emiliano, Edizioni Universitarie.

Bonini, M. (2007). Interrelations of Mud Volcanism, Fluid Venting, and Thrust-Anticline Folding: Examples from the External Northern Apennines (Emilia-Romagna, Italy), J. Geophys. Res. Solid Earth, 112, doi:10.1029/2006JB004859.

Cardellini, C., G. Chiodini and F. Frondini (2003). Application of stochastic simulation to CO2 flux from soil, Mapping and quantification of gas release, J. Geophys. Res. Solid Earth, 108, B9, 2425, doi:10.1029/2002JB002165.

Chiodini, G., F. Frondini and F. Ponziani (1995). Deep structures and carbon dioxide degassing in Central Italy, Geothermics, 24, 81-94, doi:10.1016/0375-6505(94)00023-6.

De Nardo, M. T. (2019). Le salse dell'Emilia-Romagna: cartografie a confronto. Regione Emilia-Romagna, https://ambiente.regione.emilia-romagna.it/it/geologia/geologia/acque/risorse-montagna/salse-e-cartografia-1.

Dainelli, G. (1907). Le salse dell'Appennino settentrionale. Memorie Geografiche, 1, Suppl. Rivista Geografica Italiana.

Ferrari, G. (1876). Cronache delle salse di Nirano e dei fenomeni geologici ad esse connessi, Tipografia Reggiana.

Etiope, G., G. Martinelli, A. Caracausi and F. Italiano (2007). Methane seeps and mud volcanoes in Italy: Gas origin, fractionation and emission to the atmosphere, Geophys. Res. Lett., 34, L14303, doi:10.1029/2007GL030341.

Mazzini, A. and G. Etiope (2017). Mud volcanism: An updated review, Earth-Sci. Rev., 168, 81-112, doi:10.1016/j.earscirev.2017.03.001.

Mammino, P. (2014). I vulcani di fango di Paternò e Belpasso sul versante sud-occidentale dell' Etna, Memorie Descrittive della Carta Geologica d'Italia, 102, 2014, 171-182.

Martinelli, G. and A. Judd (2004). Mud volcanoes of Italy, Geol. J., 39, 1, 49-61, doi:10.1002/gj.943.

Minissale, A., G. Magro, G. Martinelli, O. Vaselli et al. (2000). Fluid geochemical transect in the Northern Apennines (central-northern Italy): fluid genesis and migration and tectonic implications, Tectonophysics, 316, 3-4, 199-217, doi:10.1016/S0040-1951(00)00031-7.

Pesci, A., G. Teza, F. Loddo, M. Fabris et al. (2022). Evaluation of possible systematic effects in SfM UAV based point clouds: TLS and surface variations for error mitigation methods (Studio di possibili effetti sistematici nelle nuvole di punti SfM da APR: confronti con TLS, distorsioni e metodi di mitigazione), Quaderni di Geofisica, 177, 1-22, doi:10.13127/qdg/177.

Pesci, A., G. Teza and F. Loddo (2024). Point clouds repeatability and fast scale factor estimates in free SfM surveying: terrestrial application and empirical approach, Ann. Geophys., 66, 5, doi:10.4401/ag-9009.

Sciarra, A., B. Cantucci, M. Conventi and T. Ricci (2017). Caratterizzazione geochimica e monitoraggio dei flussi e delle componenti gassose nella Riserva delle Salse di Nirano, Atti della Società dei Naturalisti e Matematici di Modena, 148 Suppl., Società dei Naturalisti e Matematici di Modena.

Silvestri, O. (1866). Le Salse e la Eruzione di Fango di Paternò (Sicilia), Osservazioni e Ricerche, Stabilimento Tipografico, C. Galatola, Catania, 1886, 3.

Spallanzani, L. (1777). Viaggio nell'Appennino: osservazioni geologiche e chimiche sui vulcani di fango, Tipografia Reggiana.

Vradi, A., C. De Luca and F. Rocca (2023). Validating the European Ground Motion Service: An Assessment of Measurement Point Density, ISPRS Archives, XLVIII, 4, 247-254, doi:10.5194/isprs-archives-XLVIII-4-W7-2023-247-2023.

***CORRESPONDING AUTHOR: Arianna PESCI**,
Istituto Nazionale di Geofisica e Vulcanologia, Sezione di Bologna, Bologna, Italy
e-mail: arianna.pesci@ingv.it